ACS Sustainable Chemistry & Engineering

pubs.acs.org/journal/ascecg

Research Article

Synthesis of Bio-Based Repairable Polyimines with Tailored Properties by Lignin Fractionation

Di Xie, Yunqiao Pu, Nathan D. Bryant, David P. Harper, Wei Wang, Arthur J. Ragauskas, and Mi Li*

Cite This: *ACS Sustainable Chem. Eng.* 2024, 12, 6606−6618

Read Online

ACCESS | Metrics & More | Article Recommendations | Supporting Information

ABSTRACT: Developing sustainable polymers with low-value lignin remains a challenge. Herein, lignin-containing repairable polyimines were synthesized with tailored properties using lignin fractionation. First, softwood Kraft lignin is fractionated into a more homogeneous fraction with a lower molecular weight and a higher OH content. Next, Kraft lignin and its fraction are esterified by levulinic acid to introduce active ketone groups and subsequently condensed with oleylamine (OAm) and bis(3-aminopropyl)-terminated polydimethylsiloxane (PDMS) *via* a catalyst-free Schiff-base reaction to form grafted lignin-OAm copolymers and cross-linked lignin-PDMS polymer networks (MKL-P and MFL-P), respectively. Results show that lignin-OAm polyimines can be self-repaired and hot reprocessed under pressure, while lignin-PDMS polyimines can be repaired with the assistance of a healing agent, heat, and pressure. Dynamic mechanical analyses demonstrate that the stress−relaxation behaviors of the polyimines follow the Arrhenius law under thermal-stress activation, indicating the occurrence of transimination. Moreover, compared with Kraft lignin, the lignin fraction ameliorates the grafting density of ketones and enhances the cross-linking density of lignin-PDMS polyimine networks. The higher cross-linking density of MFL-P leads to superior stress−relaxation activation energy, thermal stability, hydrophobicity, and light-shielding ability but inferior repairability and translucency. This work provides insights into the polymerization of lignin-based polymer networks and the potential application of lignin-PDMS polyimines for repairable, translucent, anti-UV, and hydrophobic coatings.

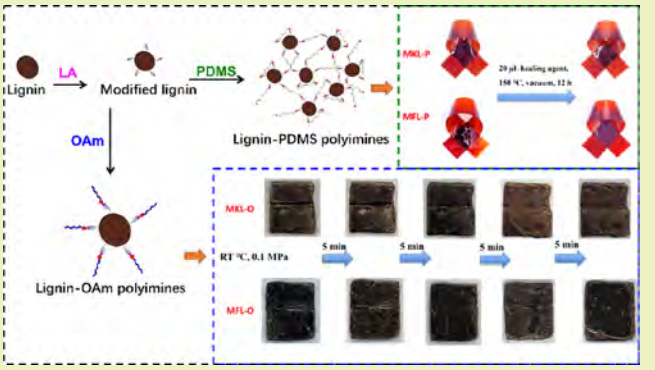

KEYWORDS: *lignin, polyimines, repairability, dynamic imine bond, cross-linking polymer network*

INTRODUCTION

To promote a green, sustainable, and circular economy, researchers are dedicated to developing chemically recyclable polymers using bioderived polymers as a partial replacement to be applied in manufacturing industries.[1−3] One promising avenue is to prepare novel dynamic covalent polymer networks (DCPN), which typically can be chemically recycled (repaired, reshaped, and reprocessed) *via* dynamic chemistries such as transimination, transesterification, andtranscarbamoylation etc.[4] The reversible reaction between amines and ketones/aldehydes is one of the most common reactions to construct robust molecules by the formation of covalent imine bonds in organic chemistry.[5] The imine bonds can break and reform simultaneously under triggers like heat, pressure, excessive free amines, catalysts, or a solvent *via* imine metathesis and exchange reactions.[4−6]

In terms of the DCPN developed by dynamic imine bonds, vanillin is a widely investigated bioderived feedstock[7,8] due to the aldehyde group that allows for imine condensation, the capability of monomer recovery, and the retaining of high-performance properties.[9] However, one vanillin molecule could participate in only one imine condensation due to the singular aldehyde group per molecule. Therefore, to obtain vanillin-based polyimines with highly cross-linked networks with favorable thermomechanical properties, vanillin is usually premodified to enrich the content of aldehydes and afterward cross-linked with multiamines.[7,8,10]

Apart from vanillin, bioderived materials such as lignin, cellulose, and vegetable oil also offer renewable alternatives to petroleum-based precursors commonly used in DCPN synthesis.[6,11,12] Lignin is one of the most challenging bioderived feedstocks to be utilized because of its poor compatibility/dispersity in solvent, structural heterogeneity, and molecular rigidity.[13,14] Nevertheless, lignin still attracts great attention due to its high abundance, low cost, rich reactive sites, good

Received: December 23, 2023
Revised: March 24, 2024
Accepted: March 26, 2024
Published: April 12, 2024

https://doi.org/10.1021/acssuschemeng.3c08482
ACS Sustainable Chem. Eng. 2024, 12, 6606−6618

thermal stability, ultraviolet (UV)-shielding ability, and biodegradability.[15] Kraft lignin (KL), a byproduct of the pulp and paper industry, represents a readily available and inexpensive resource.[16] The unique chemical structures of KL comprise a variety of functional groups, including (phenolic, aliphatic, and carboxylic) hydroxyl (OH), methoxy, and carbonyl, providing abundant reactive sites for polymerization reactions.[17] In addition, the structural heterogeneity of KL, resulting from its complex chemical structures, cooking processes, and plant sources, provides opportunities for tailoring the structures and properties of the synthesized polymers.[14,18] More importantly, lignin features a natural three-dimensional polymer network with rich reactive sites ready for modification, making lignin a great candidate to act as a natural cross-linker for developing the DCPN.

Lignin, as a bioderived component, has been widely investigated to develop novel DCPN (defined as biobased DCPN) by integrating with multiple polymers, such as polyurethane,[19] poly(ethylene glycol)-epoxy,[20] and polyolefin[21] etc. For example, a mechanically strong polyurethane was catalytically synthesized with lignin and petroleum-derived polyols *via* dynamic (covalent) cross-linking networks and (noncovalent) interfacial hydrogen bonds, which could maintain excellent mechanical strength after being hot reprocessed.[22] In addition, a novel thermoset was catalytically synthesized with lignin and epoxy *via* dynamic transesterification with adequate coating hardness and adhesion performances, which could be removed by mild alkaline solution and repaired with the assistance of glycol.[20] In addition, a new class of strong, tough, and ductile thermoplastic elastomers was constructed using lignin and a modified polyolefin elastomer with the help of zinc chloride by dynamic coordination and interfacial bonds, which could remember the shape with fixing and recovery ratios up to 94 and 82%, respectively.[21] The studies give us insight into the idea that lignin is feasible and promising for constructing high-performance chemically recyclable DCPN . However, those DCNPs usually demand external stimuli of nondegradable metallic catalysts to activate the dynamic reactions. Therefore, catalyst-free activation of lignin-based DCNP is highly attractive because the absence of a catalyst eliminates the need for hazardous and refractory materials, simplifying the synthesis procedure and reducing the environmental impact.

Based on our prior study, lignin structures affect the copolymerization with poly(ε-caprolactone) due to the heterogeneous molecular weight (MW) and OH concentrations.[14] In the present study, the OHs, as grafting sites, could also affect the modification efficiency of lignin, thus influencing the polymerization with amines. Therefore, lignin was fractionated into a more homogeneous fraction with a lower MW and more OHs to fine-tune the structures and properties of the prepared polyimines. I A long-chain primary alkylamine (oleylamine, OAm) and a bis(3-aminopropyl)-terminated poly(dimethylsiloxane) (PDMS) were selected to condense with lignin because of their versatility, flexible chains, low-surface energy, and other advantageous features for the consideration of further applications for hydrophobic coatings,[23,24] which is expected to improve the film-forming ability, hydrophobicity, and other coating performances of lignin.[25] To enable the polymerization between lignin and amines, lignin was firstly modified with sustainable levulinic acid (LA) to introduce active ketone groups.[26] OAm and PDMS, terminated with mono- and biprimary amines, respectively, would react with ketones in the modified lignin *via* Schiff-base reactions. However, the type and complexity of the polymerization with lignin are hypothesized to be different between OAm and PDMS: (1) The reaction with OAm is expected to be more feasible than that with PDMS due to the smaller steric hindrance, and (2) the polymerization types are supposed to vary due to the different amounts of terminated amines/molecule. We hypothesize that lignin-OAm polyimines will afford grafting-polymerized thermoplastic-like properties, while lignin-PDMS polyimines are prone to be cross-linking-polymerized thermosets. Branched polyimines and cross-linked polyimine networks are therefore be formed *via* a Schiff-base reaction between modified lignin and OAm and PDMS, respectively.[14]

EXPERIMENTAL SECTION

Materials. Indulin AT softwood KL was provided by MeadWestvaco (Richmond, VA, USA). LA, dimethyl sulfoxide (DMSO), 4-dimethylaminopyridine (DAP), *N*,*N*′-dicyclohexylcarbodiimide (DCC), OAm, PDMS (number-average molecular weight (M_n): ∼2,500 Da), deuterated DMSO (DMSO-d_6), toluene, methanol, acetone, hexane, acetic anhydride, tetrahydrofuran (THF), 2-chloro-4,4,5,5-tetramethyl-1,3,2-dioxaphospholane (TMDP, 95%), *N*-hydroxy-5-norbene-2,3-dicarboxylic acid imide (NHND), nonane, octane, heptane, acetonitrile, ethyl acetate, and dichloromethane were purchased from MilliporeSigma (St. Louis, MO, USA). Anhydrous pyridine was purchased from Spectrum Chemical (New Brunswick, NJ, USA). The filter paper (coarse porosity, qualitative: P8) was purchased from Fisher Scientific (Pittsburgh, PA, USA). All chemicals and materials were used as received.

Lignin Fractionation and Modification. Fractionated lignin (FL, yield: 75.8%) was obtained by solvent fractionation of KL using acetone/methanol/ (7:3, v/v) as a cosolvent and hexane as an antisolvent (Figure S1).[27] KL and FL were modified by LA to graft ketone groups using a reported method.[26] Briefly, KL (20 g, 111.2 mmol of OH), LA (19.34 g, 166.8 mmol of COOH), and DAP (1.36 g, 11.12 mmol) were dissolved in 500 mL DMSO solvent. The DCC (25.24 g, 122.32 mmol)/DMSO solution (30 mL) was then added dropwise and reacted at room temperature (RT) for 48 h. Next, the condensed liquid phase of the reaction product was obtained by successive filtration and rotary evaporation and then precipitated in 50% methanol aqueous solution followed by filtration to obtain modified KL (MKL). Modified FL (MFL) was prepared with the same procedure as MKL, during which 20 g of FL (123.4 mmol of OH), 21.46 g of LA (185.1 mmol of COOH), 1.51 g of DAP (12.34 mmol), 28.01 g of DCC (135.74 mmol), and 30 mL of DMSO were used. MKL and MFL were successively washed with deionized water three times to remove solvents and vacuum-dried for later use. The yields of MKL and MFL were 66.8 and 68.7%, respectively, which are comparable with the yield (64.3%) in the previous report.[26] The OH decreasing percentage was calculated as the molar ratio of consumed phenolic and aliphatic OH in modified lignin (MKL and MFL) to the total available phenolic and aliphatic OH in lignin (KL and FL) (eq 1) based on the ^{31}P NMR quantification results (Table S1) under the assumption that only aliphatic and phenolic OHs in KL and FL participated in the esterification with the COOH in LA. The content of ketones in modified lignin is calculated as the reduced aliphatic and phenolic OH after LA modification.

$$\text{OH decrease percentage} = \left(1 - \frac{C_{\text{OH,ML}}}{C_{\text{OH,L}}}\right) \times 100\% \quad (1)$$

where $C_{\text{OH,ML}}$ is the sum of contents of aliphatic and phenolic OH in modified lignin and $C_{\text{OH,L}}$ is the sum of contents of aliphatic and phenolic OH in the unmodified lignin.

The ketone grafting density is calculated by eq 2:

$$\text{ketone grafting density} = (M_{\text{ML}} - M_{\text{L}})/98 \text{ g/mol} \quad (2)$$

https://doi.org/10.1021/acssuschemeng.3c08482
ACS Sustainable Chem. Eng. 2024, 12, 6606−6618

where M_{ML} and M_L are the M_w of modified lignin and unmodified lignin, respectively; 98 g/mol is the increment molecular weight of a single grafted LA chain.

Synthesis of Lignin-Based Polyimines. The preparation of lignin-based polyimines was conducted as follows. First, MKL (1 g, ∼3.99 mmol of ketone groups) and MFL (1 g, ∼4.77 mmol of ketone groups) were fully dissolved in 50 mL of THF, respectively. Then, OAm or PDMS with a ketone/amine group molar ratio of 1:1 was added dropwise to the lignin/THF solutions, respectively. The mixture was prereacted at 80 °C for 24 h *via* a Schiff-base reaction. Subsequently, the products were poured into an aluminum dish (inner diameter: 114 mm) for solvent evaporation at RT overnight in a fume hood to yield gel-like films. The films were cured and postcured under 130 and 150 °C in a vacuum oven for 12 h, respectively, to obtain film-shape polyimines. The lignin-OAm and lignin-PDMS polyimine films were named MKL-O, MFL-O, MKL-P, and MFL-P, respectively. The thicknesses of the lignin-OAm (MKL-O and MFL-O) and lignin-PDMS (MKL-P and MFL-P) polyimine films are ∼1 and ∼0.3 mm, respectively.

Characterization of Lignin, Modified Lignin, and Lignin-Based Polyimines. The weight-average molecular weight (M_w), M_n, and molar-mass dispersity ($Đ_M$) of lignin, modified lignin, and polyimines were measured by gel permeation chromatography (GPC) using an Agilent 1200 HPLC system (Agilent Technologies, Inc., Santa Clara, CA, USA) equipped with water Styragel columns (HR1, HR2, and HR6; Waters Corporation, Milford, MA, USA) and an ultraviolet detector (wavelength: 270 nm). The mobile phase was THF that flowed at a rate of 0.5 mL/min. Polystyrene was used as the calibration standard. KL and FL samples were acetylated to be fully dissolved in THF for the GPC measurements referring to our previous study,[14] while modified lignin and synthesized polyimines were dissolved in THF under shaking at 60 °C for 72 h. Lignin-PDMS polyimines were partially dissolved in THF (gel fraction: MKL-P = 48.9% and MFL-P = 67.6%) with soluble portions used for GPC measurements.

The structural features of lignin, modified lignin, and polyimines were characterized by Fourier transform infrared spectroscopy (FTIR), ^{1}H nuclear magnetic resonance (NMR), ^{31}P NMR, and ^{13}C NMR. FTIR spectra of samples were recorded by an FTIR spectrometer (Spectrum One FTIR system, PerkinElmer, Wellesley, USA) with a universal attenuated total reflection accessory under wavenumbers using 4,000 to 600 cm^{-1} with a resolution of 4 cm^{-1} for 32 scans. Samples were dissolved in DMSO-d_6 at a concentration of 100 mg/mL for the acquisition of NMR spectral data using a Bruker Avance III HD 500 MHz spectrometer (Bruker, Switzerland) equipped with a 5 mm N_2 cryogenically cooled BBO H&F probe. One-dimensional "zg30" and "zgpg" pulse sequences were employed for ^{1}H NMR and ^{13}C NMR spectra, respectively. The lignin-OAm and lignin-PDMS polyimines were dissolved in DMSO-d_6 under shaking at 60 °C for 24 and 72 h, respectively. Lignin-OAm polyimines were fully dissolved, while lignin-PDMS polyimines were partially dissolved in DMSO-d_6 (gel fraction: MKL-P = 65.4% and MFL-P = 82.5%) with soluble portions used for NMR measurements. The number of scans is 16 for the acquisition of ^{1}H NMR spectra, 1024 × 2 for ^{13}C NMR spectra of lignin, modified lignin, and lignin-OAm polyimines, and 1024 × 16 for ^{13}C NMR spectra of lignin-PDMS polyimines. An inverse-gated decoupling pulse sequence "Waltz-16" was used for ^{31}P NMR experiments to quantify the OH contents of samples using NHND as an internal standard and TMDP as a phosphitylation agent.[28] The acquired spectra were processed by using Bruker Topspin 3.5 software.

The solvent stability of lignin-OAm polyimines and the gel fraction (cross-linking degree) of lignin-PDMS polyimines were evaluated according to previous studies with minor modifications.[24,29] In brief, polyimine films (∼1 × 1 cm, vacuum-dried mass: m_0) were soaked in 10 mL of five different solvents, i.e., toluene, acetone, THF, DMSO, and water, at RT and 60 °C for 24 h. Next, the films were taken out on a filter paper to remove extra solvent on the surface and then vacuum-dried at 100 °C overnight to completely remove the solvents. The oven-dried mass was recorded as m_1. The solvent stability/gel fraction was calculated (eq 3) below. The solvent stability and gel fraction are used to denote lignin-OAm and lignin-PDMS polyimines, respectively. Each sample was measured twice with the means and standard deviations recorded. The solvent stability/gel fraction of films that were fully dissolved or unable to preserve the shape after the immersion was recorded as 0.

$$\text{solvent stability/gel fraction (\%)} = 100\% \times m_1/m_0 \tag{3}$$

Thermogravimetric analysis (TGA) was conducted using a Q-50 thermogravimetric analyzer (TA Instruments, USA) by the combustion of samples from 30 to 800 °C at a rate of 20 °C/min under N_2. The heating temperatures against weight losses of samples during the combustion that are recorded as TGA curves and differential TGA curves (DTG) were analyzed by Universal Analysis 2000 software. Differential scanning calorimetry (DSC) was carried out using a Q-2000 differential scanning calorimeter (TA Instruments, USA). About 5 mg of each sample was hermetically sealed in an aluminum pan and afterward subjected to a heating and cooling cycle twice, from −80 to 200 °C, at a rate of 10 °C/min under a N_2 atmosphere. The second scanning DSC heating and cooling curves were used to determine the glass transition temperature (T_g).

The stress−relaxation behaviors of modified lignin and synthesized polyimines were measured by a rotational rheometer (ARES-G2, TA Instruments, USA) equipped with 8 mm parallel-plate geometry. The polyimine films with a thickness of ∼300 μm were cut into a circle shape with a diameter of 1 cm to fit the geometry. The stress−relaxation steps were tested under different temperatures (100−200 °C) after equilibrations of temperature and geometry gaps for at least 5 min. An external axial force of 2 N and a strain of 1.5% were applied to the films. The stress−relaxation curves of the modulus as a function of time were recorded. The Arrhenius law is fitted by eq 4[20] below:

$$\ln \tau^* = \frac{E_a}{RT} - \ln A \tag{4}$$

where τ^* is the time (s) that it takes for samples to relax to 1/e (∼37%) of their initial modulus, E_a is the activation energy (the minimum energy required for chemical reactions to occur, kJ/mol), R is the ideal gas constant (∼8.315 J/(mol·K)), T is the absolute temperature (K), and A is the pre-exponential factor.

The dispersive (γ_d) and specific (γ_{sp}) surface energies of lignin, modified lignin, and polyimines were measured by an inverse gas chromatography (iGC) surface energy analyzer (SEA) equipped with a flame ionization detector (Surface Measurements Systems, Ltd., Alperton, UK). Nonpolar (nonane, octane, heptane, and hexane) and polar (acetone, ethanol, acetonitrile, ethyl acetate, and dichloromethane) probe molecules were injected successively under surface coverage from 0.01 to 0.4 n/n$_m$. Data were analyzed by advanced SEA analysis software (Advance version 1.4.2.0). The static water contact angle (WCA) of polyimine films was measured by using a contact angle goniometer (Ramé-Hart Instrument Co., USA).

The UV-blocking ability of films was evaluated by using UV−vis spectra as a function of the light wavelength (ranges from 200 to 800 nm) against transmission recorded by an Evolution 60S UV−vis spectrometer (Thermo Fisher Scientific, USA).

Repairability of Synthesized Polyimines. The repairability of the polyimines was measured by referring to a previous study.[20] Briefly, the surface of polyimine films was scratched by a razor blade, and the damaged surface of MKL-O and MFL-O polyimine films was repaired by pressing them under a flat plate with a pressure of 0.1 MPa. The damaged surface of MKL-P and MFL-P polyimine films was repaired at 150 °C in a vacuum oven for 12 h after a healing agent was filled to the damaged gaps. The healing agent was prepared by prereacting modified lignin and PDMS in THF at 80 °C for 12 h. The optical microscopy images of the damaged surface were taken before and after the repair to make comparisons using a BX51 optical microscope (Olympus, Bartlett, TN, USA).

https://doi.org/10.1021/acssuschemeng.3c08482
ACS Sustainable Chem. Eng. 2024, 12, 6606−6618

RESULTS AND DISCUSSION

Lignin Fractionation and Modification. It has been a historical challenge to utilize KL on a large scale because the structural heterogeneity of KL will affect the KL-based polymers or composites.[30] To investigate the effect of lignin structural nonuniformity on the synthesized polymers, a more homogeneous ($Đ_M$: 2.02 vs 2.98) and lower-MW (M_w: 2.167 kDa vs 4.659 kDa) FL is fractionated from KL with a yield of 75.8% (Figure S1 and Table 1). From the OH quantification results by ^{31}P NMR analysis, the concentrations of phenolic, aliphatic, carboxylic, and total OH between FL and KL vary (Table S1), which will influence further lignin modification and synthesis reactions.

Table 1. Weight-Average (M_w) and Number-Average (M_n) Molecular Weight and Molar-Mass Dispersity ($Đ_M$) of Lignin, Modified Lignin, and Lignin-Based Polyimines[a]

	M_w (kDa)	M_n (kDa)	$Đ_M$
PDMS	5.463 ± 0.034	2.983 ± 0.023	1.83 ± 0.00
	Lignin and modified lignin		
KL	4.659 ± 0.241	1.566 ± 0.039	2.98 ± 0.23
MKL	5.359 ± 0.418	1.120 ± 0.042	4.78 ± 0.20
FL	2.167 ± 0.099	1.071 ± 0.019	2.02 ± 0.06
MFL	3.603 ± 0.0485	1.120 ± 0.083	3.23 ± 0.20
	Polyimines		
MKL-O	6.388 ± 0.721	2.150 ± 0.055	2.98 ± 0.41
MFL-O	6.486 ± 0.793	1.724 ± 0.038	3.77 ± 0.54
MKL-P	54.302 ± 1.680	26.664 ± 1.113	2.04 ± 0.02
MFL-P	113.144 ± 21.531	100.915 ± 10.514	1.11 ± 0.10

[a]Note: MKL-P and MFL-P were measured only for the partially THF-dissolved portion under shaking at 60 °C for 72 h.

To enable the functionality of KL reactive sites, chemical modifications such as esterification, hydroxylation, amination, etc. are typically required.[31−33] In the current study, lignin is esterified with LA to introduce active ketone groups allowing for the Schiff-base reaction with amines (Figure 1).[26] GPC, FTIR, ^{1}H NMR, ^{13}C NMR, and ^{31}P NMR analyses prove that KL and FL are successfully modified with the following observations: (1) the M_w values of modified lignins are increased compared with the corresponding lignins (Table 1), which is attributed to the grafted LA and/or removal of low-MW lignin during methanol purification;[26] (2) the new signals of ketone groups at 1710 cm^{-1} is identified in the FTIR spectra of modified lignins (Figure S2);[6,26] (3) the new signals of methylene (signals a and b at ∼2.73 ppm) and methyl (signal c at ∼2.12 ppm) in LA are identified in the ^{1}H NMR spectra of modified lignins[26] (Figure S3); (4) the new signal of ketone (signal C_d at 206.9 ppm) is observed in the ^{13}C NMR spectra of modified lignins (Figure S4);[26] (5) the signals of aliphatic OH, guaiacyl phenolic OH, and *p*-hydroxyphenyl OH disappear, and the signal intensity of C_5-substituted OH apparently recedes in the ^{31}P NMR spectra of modified lignins (Figure S5). The reduced content of aliphatic OHs and phenolic OHs in modified lignins (Table S1) is attributed to the esterification with the carboxyl of LA.[26] There are ∼26% aliphatic and 22% phenolic OH remaining in MKL and ∼17% aliphatic and ∼16% phenolic OH remaining in MFL,

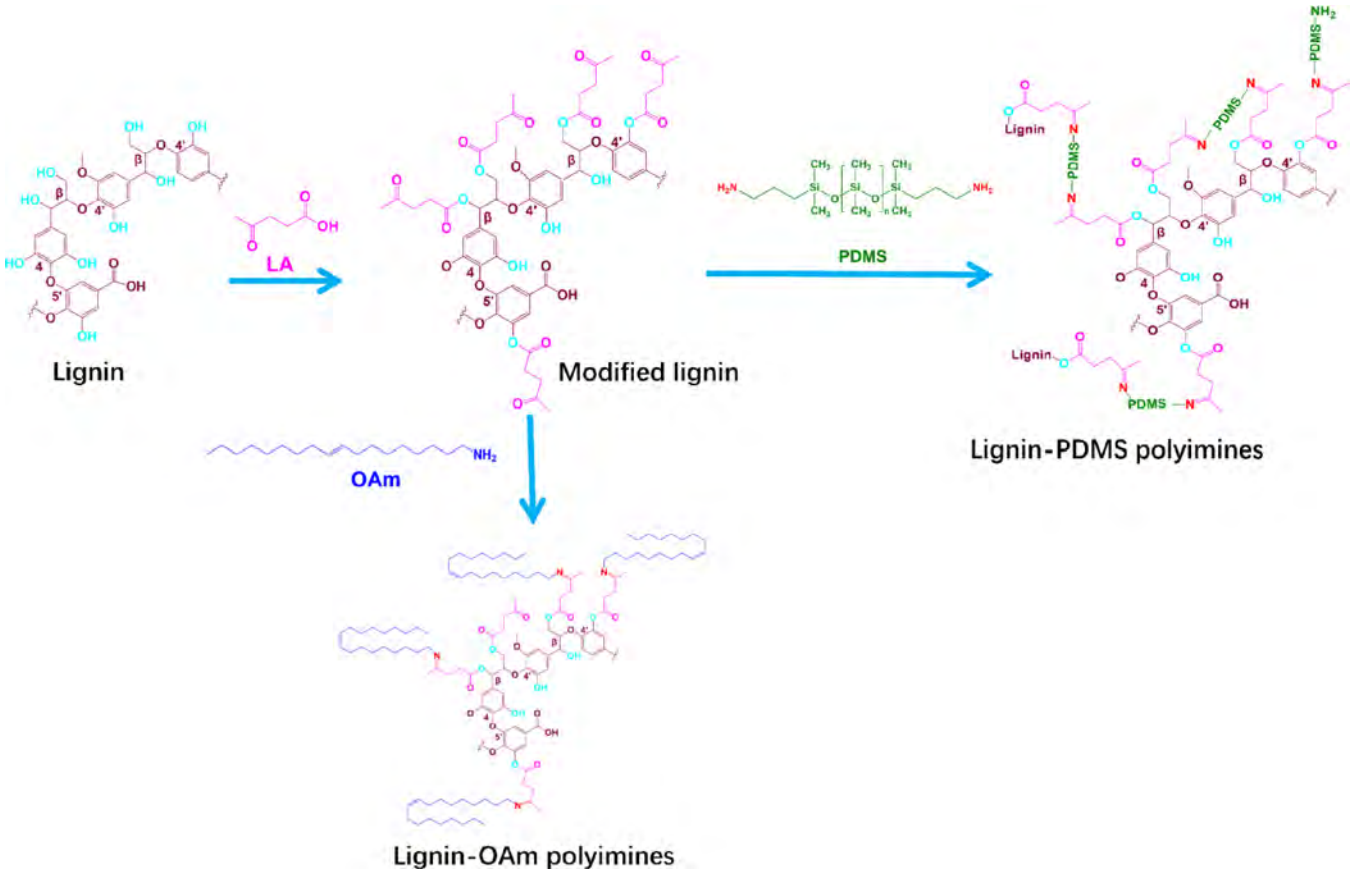

Figure 1. Proposed mechanisms of lignin modification and polyimine synthesis.

https://doi.org/10.1021/acssuschemeng.3c08482
ACS Sustainable Chem. Eng. 2024, 12, 6606−6618

compared with unmodified lignin (Table S1). The reasons could be that (1) the OHs in lignin were not fully esterified by LA. It is worth noting that compared with MKL, the ketone grafting density of MFL is approximately twice as many as that of MFL (14.65 vs 7.14), which is likely on account of the higher amount of OHs and lower MW of FL that favor the LA esterification.[14] Moreover, from Figure S4, the intensity of the chemical shift of C_a (ester) in MFL is stronger than that in MKL, which is attributed by the fact that at a concentration of 100 mg/mL, the MFL/DMSO-d_6 solution contains more ester groups than the MKL/DMSO-d_6 solution because of the higher ketone grafting density (14.65 vs 7.14) and lower M_w (3.603 kDa vs 5.359 kDa) of MFL. However, there might be a rare occurrence of intramolecular and intermolecular esterification among lignin molecules[26] because the COOH content in both MKL (0.08 vs 0.32 mmol/g) and MFL (0.09 vs 0.46 mmol/g) is decreased compared with KL and FL, respectively (Table S1).

Synthesis and Characterization of Polyimines. Imine chemistry is one of the few synthetic strategies to construct robust molecules with chemical recyclability due to the formation of dynamic covalent bonds.[4,5] Lignin is a widely used bioderived precursor for the synthesis of high-performance polymers or DCPN due to the abundant functional groups.[34] Herein, lignin-OAm and lignin-PDMS polyimines are successfully synthesized *via* a catalyst-free Schiff-base reaction between ketones in the modified lignin and amines in OAm and PDMS (Figure 1). GPC, FTIR, and ^{13}C NMR analyses confirm the successful synthesis of polyimines. First, the tested M_w of MKL-O, MFL-O, MKL-P, and MFL-P is significantly augmented compared with the corresponding MKL and MFL (Table 1). It can also be assumed that the actual M_w of MKL-P and MFL-P is higher than the tested values (54.302 ± 1.680 and 113.144 ± 21.531 kDa) due to the partial dissolution (the undissolved portion was not reflected in the chromotographic analysis). Second, the newly formed C═N bonds are detected at around 1,660 cm^{-1} in the FTIR spectra of MKL-O, MFL-O, MKL-P, and MFL-P[6,26] (Figure 2). Lastly, the ^{13}C NMR spectra verify the formation of the

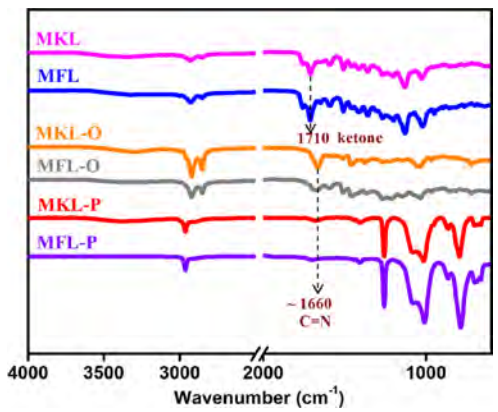

Figure 2. FTIR spectra of modified lignin and lignin-based polyimines

C═N bonds (signal C_d at ~164 ppm) in lignin-OAm polyimines and (signal C_d at 168.5 ppm) in MKL-P (Figure 3).[26,35] With a similar method to calculate LA (ketone) grafting density based on the GPC results (eq 2 and Table 1), the OAm grafting density is 4.13 for MKL-O and 11.58 for MFL-O. Combined with the calculated ketone grafting density of MKL (7.14) and MFL (14.65), the OAm grafting efficiency of MKL-O and MFL-O is 57.8 and 79.0%, respectively. The results are verified by the peak integral ratio of C_a (ester) to C_d (imine) in the ^{13}C NMR spectra of MKL-O (52.5%) and MFL-O (69.2%) (Figure 3). For lignin-PDMS polyimines, the peak integral ratio of C_a (ester) to C_d (imine) in the ^{13}C NMR spectra MKL-P is ~1.07; however, the imine bond was not detected in ^{13}C NMR spectra of MFL-P, which is attributed to its poor dissolution in DMSO-d_6 caused by the high MW. The solid-state ^{13}C NMR spectra exhibit weaker and broader but identifiable signals of C═N bonds (C_d at 160−170 ppm, Figure S6) in MKL-P and MFL-P due to the immobility of molecules under scanning.

The better solubility of lignin-OAm than lignin-PDMS polyimines agrees with the noticeably larger tested M_w of the latter than the former, which suggests that OAm with a singular amine group was grafted to modified lignins to form branched copolymers with modified lignins as skeletons and OAm as arms, while PDMS with double amine groups was cross-linked with modified lignins to form lignin-PDMS polymer networks. In addition, comparing MKL-based and MFL-based polyimines, the latter shows a higher testable M_w (Table 1), implying that lignin fractionation favors the grafting and cross-linking polymerization with amines. It could be attributed to the enhanced reactive (phenolic and aliphatic) OH sites in FL (Table S1), reduced steric hindrance effect of lower-M_w MFL,[36] and the increased ketone grafting density of MFL compared with MKL in the current study. As for the lignin-OAm polyimines, the $Đ_M$ is slightly decreased compared with the modified lignin prior to the imine condensation (Table 1), which could be related to the negative relationship between the content of active OHs and lignin MW.[27] It means higher-MW lignin tends to have less LA and OAm grafted arms and vice versa, thus narrowing the MW distribution of synthesized lignin-OAm polyimines.

Physicochemical Properties of Polyimines. For the sake of future applications, it is of great significance to have a thorough understanding of the physicochemical properties of synthesized lignin-based polyimines. During the solvent stability test, MKL-P and MFL-P were swollen into transparent gels after immersing under toluene, acetone, THF, and DMSO, while no swelling occurred to MKL-O and MFL-O, which aligns with our hypothesis that lignin-PDMS polyimines are in the form of a cross-linked polymer network while lignin-OAm polyimines are in the form of grafted copolymers. Furthermore, the gel fractions of the synthetic lignin-PDMS polyimines reach over 85% after being immersed under polar solvents including acetone, DMSO, and water; however, their gel fractions are below 80% in less polar solvents including THF and toluene (Table 2). It suggests an overall nonpolarity of lignin-PDMS polyimines. Theoretically, the Schiff-base condensation reaction proceeds with water as a byproduct, and the reversible hydrolysis reaction will proceed at the presence water molecules,[5,37] which could lead to humidity instability. However, in the current study, the gel fractions of lignin-PDMS polyimines are 100% after immersion under water for 24 h at RT (Table 2). We reason that it may be related to the facts that (i) the incorporation of low-surface-energy PDMS restrains the water uptake to the polyimines, (ii) the hydrophobic functional groups in lignin (like aromatics and esters and the long-chain alkyls in OAm) prevent water from penetrating the polymers, and (iii) the compact structures of covalent cross-linking polymer networks of lignin-PDMS

https://doi.org/10.1021/acssuschemeng.3c08482
ACS Sustainable Chem. Eng. 2024, 12, 6606−6618

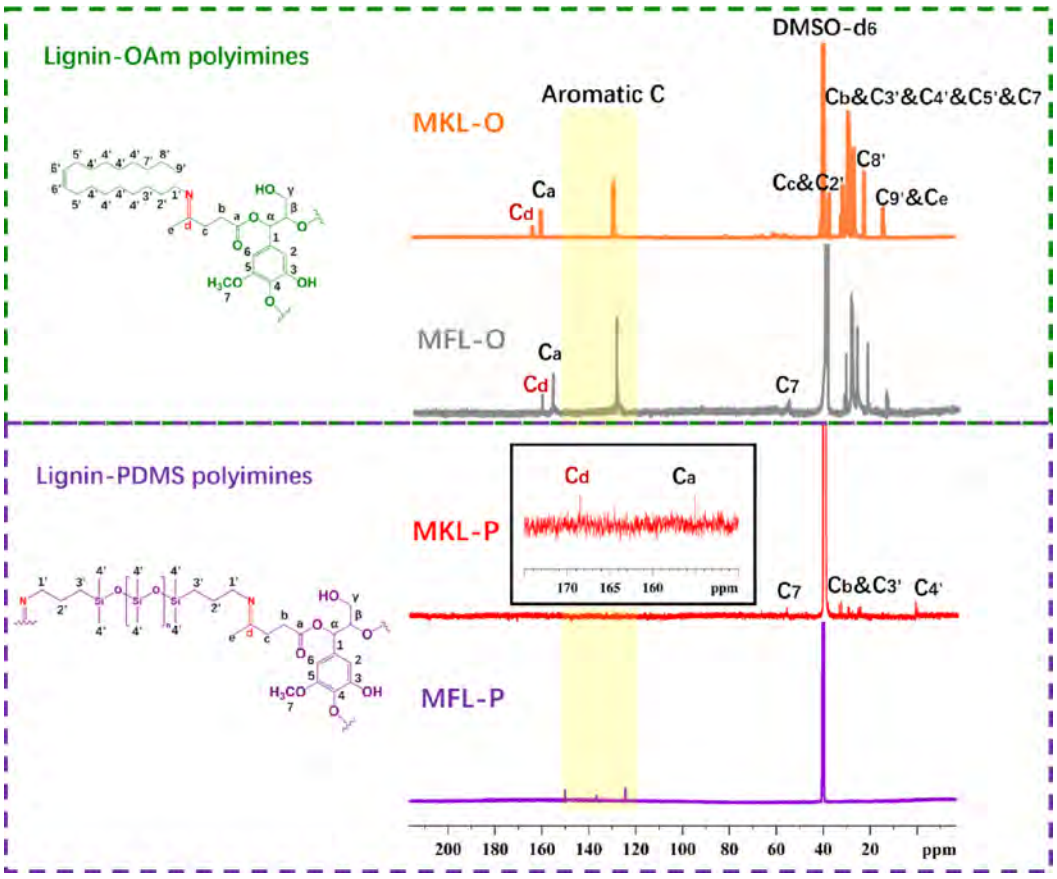

Figure 3. ^{13}C NMR spectra of lignin-based polyimines with DMSO-d_6 as a solvent.

Table 2. Solvent Stability and Gel Fraction of Synthesized Lignin-Based Polyimines

	solvent stability (%)				gel fraction (%)			
	MKL-O		MFL-O		MKL-P		MFL-P	
solvent	25 °C	60 °C	25 °C	60 °C	25 °C	60 °C	25 °C	60 °C
toluene	35.2 ± 0.4	32.5 ± 2.5	46.9 ± 0.9	42.9 ± 0.8	78.5 ± 0.5	75.3 ± 0.3	84.5 ± 2.2	82.5 ± 0.4
acetone	74.3 ± 2.9	0	80.7 ± 2.9	0	85.2 ± 0.3	83.8 ± 0.5	91.9 ± 0.6	90.5 ± 0.5
THF	0	0	0	0	67.5 ± 1.1	58.6 ± 3.1	82.1 ± 1.6	80.1 ± 2.5
DMSO	74.5 ± 2.8	0	83.8 ± 2.2	0	87.2 ± 5.3	81.6 ± 4.0	92.1 ± 3.8	90.8 ± 3.7
H_2O	99.5 ± 0	98.4 ± 0.6	99.5 ± 0	99.1 ± 0.1	100.0 ± 0	99.9 ± 0.2	100.0 ± 0	100.0 ± 0

polyimines slow down water molecular access for imine hydrolysis, presenting the observed water stability. In addition, the gel fraction of MKL-P is lower than that of MFL-P under five tested solvents, together with the testable M_w (Table 1), indicating a higher cross-linking density of MFL-P. The higher cross-linking density of MFL-P results from the more active sites with PDMS in MFL caused by the increased ketone grafting density of FL (Table S1) and the reduced steric hindrance effect of MFL with a lower M_w (Table 1)[38] that would further lead to various physicochemical properties of the synthesized polyimines.[39]

To understand the thermal properties of lignins and the synthesized polyimines, T_g and thermal stability are characterized by DSC and TGA (Table 3 and Figure 4). Firstly, the T_g of modified lignin and polyimines is slightly different from the lignin source. Furthermore, the thermal stability of FL increases compared with KL revealed by a higher T_{max} (385 °C vs 363 °C, Table 3), which is triggered by the occurrence of less stable ether bonds and more stable C−C bonds in FL than KL after fractionation.[40] In addition, the modified lignin exhibits a broader thermal degradation range than the unmodified lignin, which is due to the more complex

Table 3. Glass Transition Temperature (T_g), Temperatures at the Onset of Thermal Degradation (T_{onset}) and Maximum Mass Loss (T_{max}), Residual Carbon Content (C_r), and Calculated Average Activation Energy (E_a) of Lignin, Modified Lignin, and Lignin-Based Polyimines

	T_g (°C)	T_{onset} (°C)	T_{max} (°C)	C_r (%)	E_a (kJ/mol)
KL	154	252	363	43.6	N/A
FL	158	261	385	40.0	N/A
MKL	154	157	342−387	27.2	N/A
MFL	152	164	326−394	25.6	N/A
MKL-O	157	222	434	11.3	43.5
MFL-O	158	251	429	16.7	44.8
MKL-P	154	325	518	7.9	100.0
MFL-P	155	385	576	29.7	130.2

https://doi.org/10.1021/acssuschemeng.3c08482
ACS Sustainable Chem. Eng. 2024, 12, 6606−6618

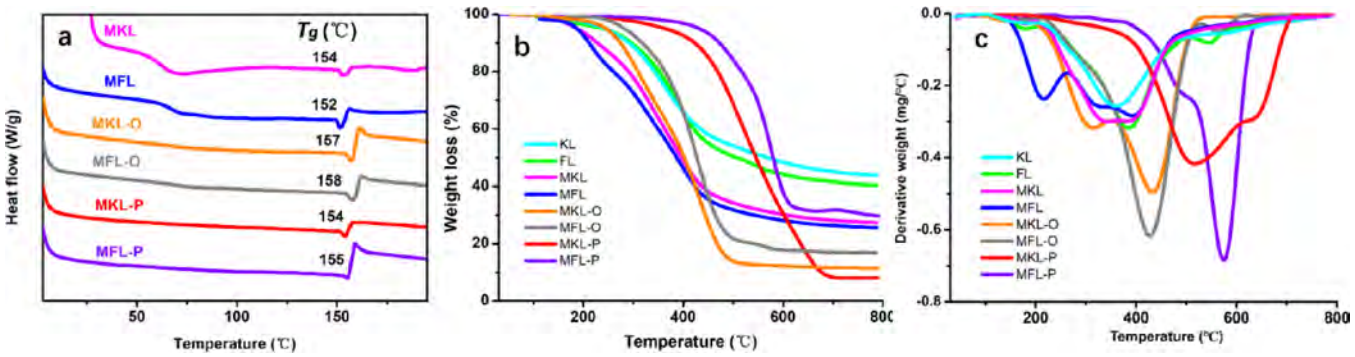

Figure 4. DSC (a), TGA (b), and DTG (c) curves of lignin, modified lignin, and lignin-based polyimines

compositions including a lignin core and grafted LA arms that lead to multiple degradation pathways.[41] Also, the thermal stability of the synthesized polyimines is much higher than the corresponding modified lignin (T_{max}: ~400 °C vs ~500 °C, Table 3), which can be explained by the introduction of thermally stable structures such as C−C and silicones and elevated MW after the polymerization. For lignin-PDMS polyimines, the dual (lignin−lignin and lignin-PDMS) cross-linking network further contributes to a higher thermal stability. Compared with MKL-P, MFL-P displays higher thermal stability (T_{max}: 576 °C vs 518 °C, Table 3), which agrees with our previous measurement of the gel fraction (Table 2) that the cross-linking density of MFL-P is higher than that of MKL-P.

Dynamic imine chemistry with reversible imine bonds can be stimulated by heat, pressure, excess primary amine, and polar solvents.[6,37] In this study, no product purification process was addressed in the protocol. Theoretically, all the amines are expected to be consumed stoichiometrically since the ketone/amine group molar ratio is pre-dosed as 1:1. However, the ketone molar amount in modified lignin is calculated based on eq 1 without considering the intermolecular and intramolecular esterification. In addition, the OAm grafting efficiency of MKL-O and MFL-O is 57.8% and 79.0%, respectively. Therefore, excess amines are present in the final products without forming imine bonds. To further confirm the associated imine bond exchanging process of synthesized polyimines, dynamic mechanical compression analysis was conducted. As a result, all four synthesized polyimines recovered their original shape and hardness after the removal of heat and stress without using a mold. They also show observable temperature-dependent stress−relaxation behaviors and follow the Arrhenius law (Figure 5), suggesting that chemical reactions took place under thermal and stress activation.[4] On the one hand, lignin-OAm polyimines are more thermoplastic-like whose relaxation modulus decreases exponentially in the early stage and tends to be constant in the late stage (Figure 5a,b), indicating that lignin-OAm polyimines are copolymers mainly consisting of noncovalent hydrogen networks that are easily overcome, and the imine bonds act as chain extenders of the lignin core.[42] On the other hand, traditional thermosets are hard to stress−relax under heating because of the irreversible covalent bonds.[20] However, in this work, the relaxation modulus of lignin-PDMS polyimines is released slowly first and significantly later (Figure 5c,d), indicating that they are adaptable thermoset-like networks mainly due to the dynamic imine covalent networks that are responsible for their stress−relaxation behavior.[43] In other words, the occurrence of imine exchange and metathesis is likely the reason for their network rearrangement and stress−relaxation behavior.[24,44] Comparing lignin-PDMS and lignin-OAm polyimines, the latter exhibits much faster relaxation rates under the same temperatures and applied strain (Figure 5), as well as a lower E_a (Table 3), which can be explained by the fact that the covalent cross-linking network of lignin-PDMS polyimines is more complex and rigid than the core-branch-shaped lignin-OAm polyimines, leading to a more difficulty in chain mobility and rearrangement and a reduced capability to dissipate stress over time.[45]

Herein, both MKL-P and MFL-P relax faster as the temperature increases (Figure 5c,d), which is due to the elevated temperature and pressure promoting the mobility and diffusion of the silicone chains, allowing for the rearrangement of imine bonds in response to the applied pressure.[24] In addition, MKL-P shows comparable E_a with reported transamination of Schiff-base bonds,[24,46,47] while MFL-P shows a higher E_a than MKL-P (Table 4), indicating that their stress−relaxation behaviors highly depend on the cross-linker, i.e., lignin. We contend that MFL-P synthesized by the more homogeneous and lower-MW FL possesses an increased covalent cross-linking density and a less flexible network than non-fractionated and larger lignin-led MKL-P, restricting the intermolecular and intramolecular mobility of the amine and imine groups, thus hampering the dynamic imine metastasis and exchange reactions and the reformation of the polymers.[44] It may also be attributed to the reduction of noncovalent interactions (H-bonding) among lignin, PDMS, and polyimines that favor the melting and reshaping of MFL-P under heat.[24] Therefore, MFL-P requires a longer time and/or higher temperature to relax.

The surface properties, including dispersive and specific surface energy, hydrophilicity index, and WCA, are also characterized. As expected, both the dispersive and specific surface energy of modified lignin are more heterogeneous (*i.e.*, the range between maximum and minimum surface energy is relatively narrow) than those of original lignin because the grafted active arms introduce more diverse functional groups and more complicated structures, whereas they become more homogeneous after the synthesis with amines because the incorporations of long-chain OAm and low-surface-energy PDMS[25] lower the maximum surface energy of modified lignin (Figure 6a,b). However, we want to point out the specifica surface area of the polyimine products in this study is very low < 1 m^2/g, which easily leads to a disparity of the surface coverage and surface energy quantification. Further verification with large samples running needs to be conducted. The

https://doi.org/10.1021/acssuschemeng.3c08482
ACS Sustainable Chem. Eng. 2024, 12, 6606−6618

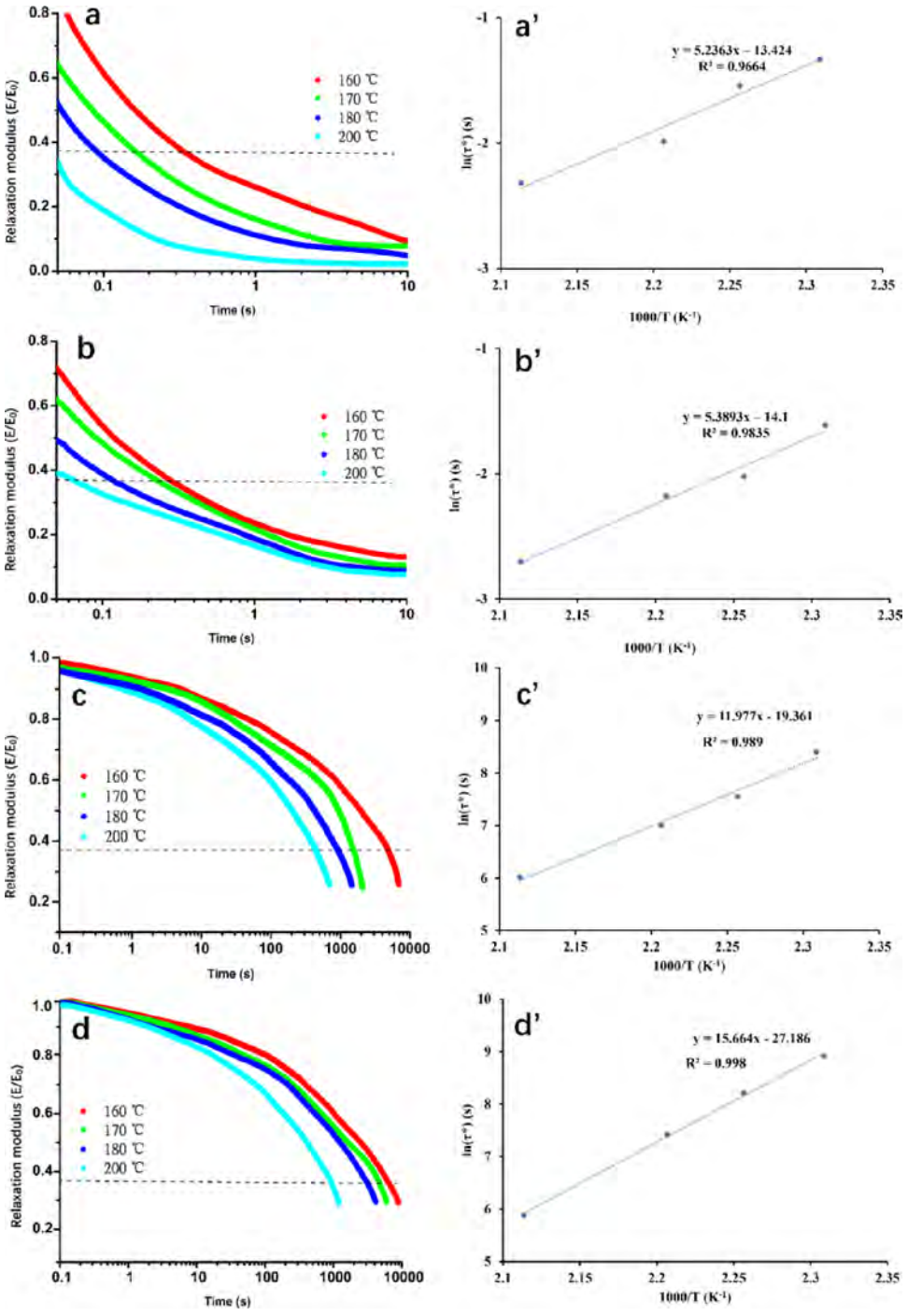

Figure 5. Stress−relaxation curves (a−d) and Arrhenius equation plots (a'−d') of MKL-O (a,a'), MFL-O (b,b'), MKL-P (c,c'), and MFL-P (d,d'). The dashed line refers to 1/e (~0.37) of the initial modulus.

decreased hydrophilic index of polyimines implies that the introduction of OAm and PDMS weakens the water affinity of modified lignin (Table 4). It is worth noting that the WCA of MFL-P reaches 111°, higher than many of the reported lignin-based hydrophobic thermosets.[2,20,48,49] Also, the WCA of MFL-P is higher than that of MKL-P (111° vs 106°), which is aligned with the hydrophilic index (0.10 vs 0.06) tested by iGC (Table 4). The difference might be attributed to the lower surface energy and higher water resistance of MFL-P caused by the higher cross-linking density. However, the WCA shows a minimal difference between the two lignin-OAm polyimines. The increased hydrophilicity index of MFL-O compared with MKL-O (0.09 vs 0.05, Table 4) may be attributed to the higher LA grafting efficiency of MFL that brought more polar moieties.

Compared with KL, FL has a relatively higher OH content ready for LA esterification (5.71 mmol/g vs 5.24 mmol/g) and a more homogeneous MW distribution ($Đ_M$: 2.98 vs 2.02). MFL has a higher OH decreasing percentage (83.54% vs 76.15%), ketone grafting density (14.65 vs 7.14), and lower M_w (3.603 kDa vs 5.359 kDa, Table 1) compared with MKL, which causes little differences in the structures and properties between MKL-O and MFL-O that modified with OAm but causes noticable differences between MKL-P and MFL-P that

https://doi.org/10.1021/acssuschemeng.3c08482
ACS Sustainable Chem. Eng. 2024, 12, 6606−6618

Table 4. Minimum, Median, and Maximum Values of γ_d and γ_{sp} as well as Hydrophilicity Index ($\gamma_{sp}/(\gamma_{sp} + \gamma_d)$) and WCA of Lignin, Modified Lignin, and Lignin-Based Polyimines

	γ_d (mJ/m^2)			γ_{sp} (mJ/m^2)				
samples	minimum	median	maximum	minimum	median	maximum	$\gamma_{sp}/(\gamma_{sp} + \gamma_d)$	WCA (deg)
KL	42.60	46.74	60.51	0.71	3.56	6.45	0.08	N/A
FL	11.63	20.10	35.57	0.17	0.71	4.38	0.04	N/A
MKL	42.19	45.57	110.20	11.27	6.81	26.99	0.15	N/A
MFL	33.08	41.88	114.05	5.74	7.92	20.15	0.19	N/A
MKL-O	0.68	21.12	23.41	0.03	1.02	2.14	0.05	99
MFL-O	0.93	28.85	39.52	0.70	2.73	3.19	0.09	98
MKL-P	39.74	43.57	46.80	3.59	4.54	5.49	0.10	106
MFL-P	2.25	12.93	59.41	0.11	0.83	10.88	0.06	111

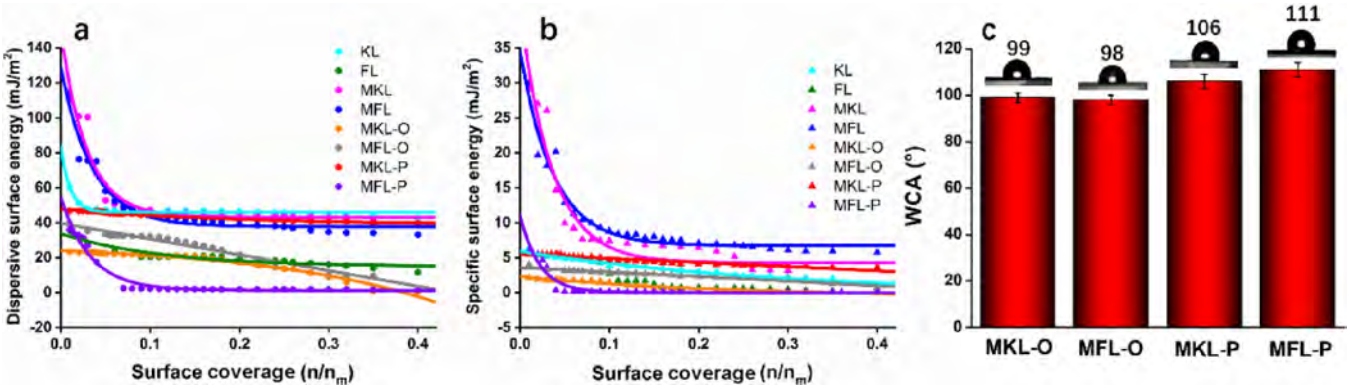

Figure 6. Dispersive (a) and specific (b) surface energy and WCA (c) of lignin, modified lignin, and synthesized lignin-based polyimines.

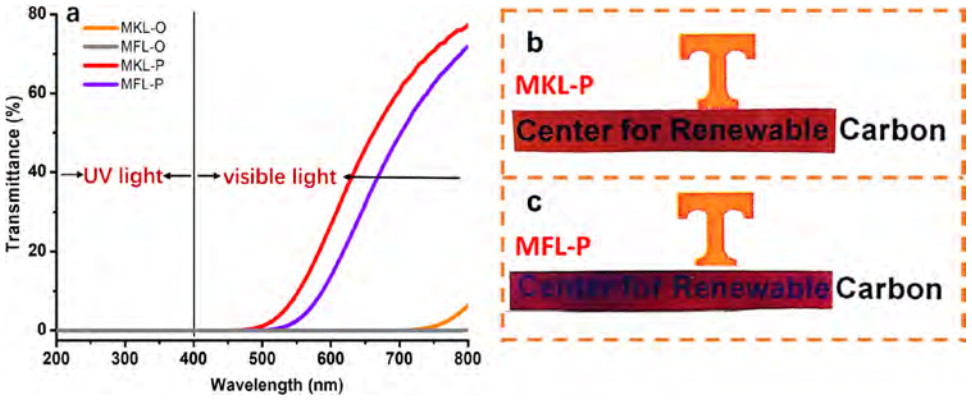

Figure 7. UV-light blocking ability (a) and images of MKL-P (b) and MFL-P (c) translucent films.

crosslined with PDMS. In particular, MFL-P possesses higher cross-linking density than MKL-P, which further leads to different thermal stability (T_{max}: 576 °C vs 518 °C, Table 3) and hydrophobicity (WCA: 111° vs 106°; hydrophobicity index: 0.06 vs 0.10, Figure 6 and Table 4). The differences are likely related not only with the amount of OH content in lignin and grafting density of LA but also the different steric hindrance of modified lignin that influences the lignin-amine polymerization.

The synthesized polyimine films exhibit a good ability to shield broad-spectrum UV radiation including UV-A (wavelength: 400−320 nm), UV−B (wavelength: 320−280 nm), and UV−C (wavelength: 280−200 nm) with 0% transmittance of UV light. Among them, lignin-OAm films exhibit a better ability to shield visible light (wavelength: 400−800 nm) than lignin-PDMS films (Figure 7a). Their UV-blocking ability mainly is attributed to the conjugated C═C double bonds, unsaturated ethylene groups, and condensed structures in lignin.[50] Moreover, synthesized lignin-PDMS polyimine films are translucent. As we can see from Figure 7b,c, the letters "Center for Renewable" could be seen through the MKL-P and MFL-P films. The transparency mainly derives from the PDMS component, and the brownish color is mainly derived from the chromophore groups such as conjugated C═C, C═O, and COOH with aromatic rings in the lignin component.[51,52] However, MKL-P displays better visuality than MFL-P, which is in accordance with the higher visible-light transmittance of MKL-P in Figure 7a. Overall, the synthesized lignin-PDMS polyimines could act as a potential candidate for translucent, anti-UV, and hydrophobic coatings.

Reprocessing Ability and Repairability of Polyimines. Imine exchange and metathesis are the two primary reactions responsible for the reprocessing ability and recyclability of polyimines without requiring catalysts.[4−6,8] In a previous

https://doi.org/10.1021/acssuschemeng.3c08482
ACS Sustainable Chem. Eng. 2024, 12, 6606−6618

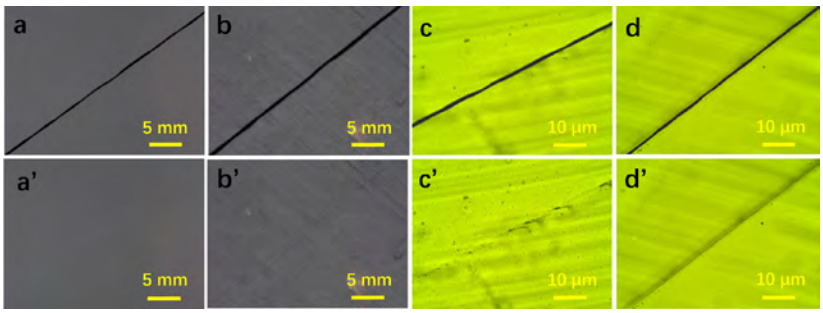

Figure 8. Optical microscopy images of MKL-O (a,a'), MFL-O (b,b'), MKL-P (c,c'), and MFL-P (d,d') before (a−d) and after (a'−d') repair.

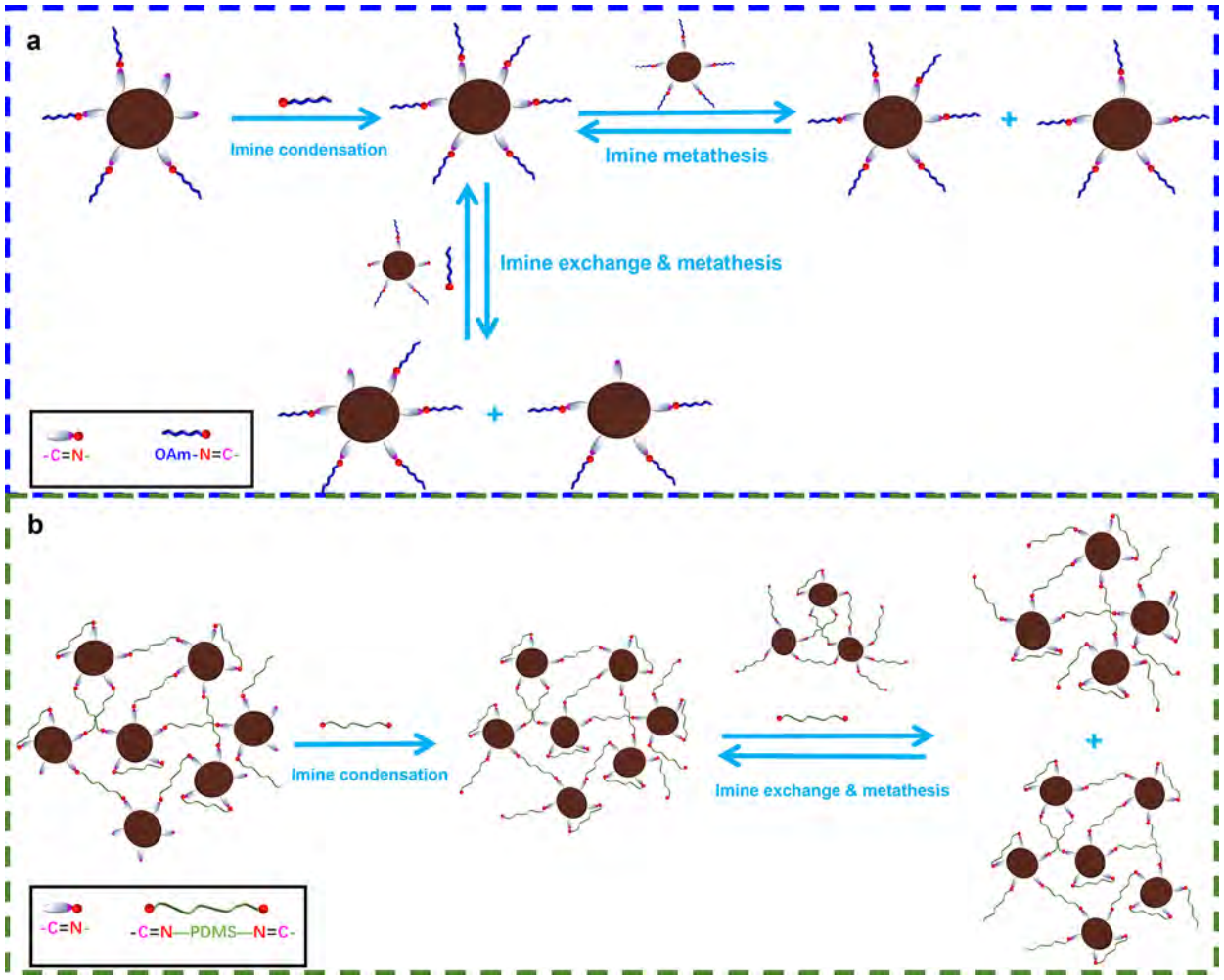

Figure 9. Proposed mechanisms of imine condensation, exchange, and metathesis reactions during the repair of lignin-OAm (a) and lignin-PDMS (b) polyimines.

report, a lignin-based polyimine thermoset was successfully reprocessed under hot press *via* dynamic imine chemistry with minimally detrimental effect on mechanical strength.[6] The dynamic imine exchange and metathesis are closely influenced by the polyimine's structures, molecular chain flexibility, and rigidity etc.[6,26] In our study, lignin-OAm polyimine films can be repurposed into new films at 160 °C and 1 MPa for 3 h after being cut into small pieces (Figure S9); however, the lignin-PDMS films are hardly reprocessed using the same procedure. It agrees with the stress−relaxation analyses that lignin-OAm polyimines are more thermoplastic-like, while lignin-PDMS polyimines are more thermoset-like.

A simple experiment testing of repairability was also conducted by reheating the razor scratches on the films under a hot press. As a result, the scratches on the lignin-OAm polyimine films could be self-healed under RT and 0.1 MPa for 20 min (Figure S10). Nevertheless, a healing agent consisted of a prereacted lignin and PDMS solution under 80 °C for 12 h was required to repair the damaged lignin-PDMS polyimine films under 150 °C and reduced pressure for 12 h (Figure S11). Under a microscale, the scratches on lignin-OAm polyimine films are nearly invisible after repair (Figure 8a',b'), while the scratches on lignin-PDMS polyimine films are repaired significantly but still observable (Figure 8c',d').

https://doi.org/10.1021/acssuschemeng.3c08482
ACS Sustainable Chem. Eng. 2024, 12, 6606−6618

Meanwhile, MKL-P appears to have better repairability than MFL-P based on the differences in the wider gap of the repaired scratche, which might be due to the higher cross-linking density of MFL-P that raises the difficulty in chain mobility and polymer rehealing.[53] Overall, lignin-OAm polyimine films can be self-healed by simply applying pressure, while lignin-PDMS polyimine films can be repaired with the help of a healing agent, heat, and pressure.

Based on with the structural characterization results, the possible dynamic bonds are imine and ester bonds in the synthesized polyimines. To investigate whether transesterification contributed to the DCPN, dynamic mechanical analyses of the esterified lignin (MKL and MFL) were also conducted. As shown in Figure S8, although MKL and MFL exhibit classic stress−relaxation behavior (viscosity−temperature dependence), the weak Arrhenius correlations (R^2 = 0.84 and 0.65, respectively) provide limited evidence for transesterification. The stress−relaxation behavior of the esterified lignin is probably attributed to the polymer melt, which rules out the contribution of transesterification to the DCPN. Therefore, dynamic imine chemistries including imine exchange and metathesis are mainly responsible for the repairability of the synthesized polyimines.

Several factors are considered to affect the dynamic imine chemistries: (1) Higher temperatures can increase the reaction rate by (i) providing more thermal energy to the reactant molecules[54] and (ii) increasing the chain mobility of the silicone,[24] thereby promoting the breaking and reformation of C═N bonds and bond rearrangement in response to heat and pressure; (2) Pressure can affect imine exchange and metathesis reactions indirectly by influencing the solubility and diffusion of reactants to impact the reaction kinetics;[55] (3) Excessive amines play an important role in initiating the dynamic imine exchange and metathesis. A prior report investigated that the amine concentrations affect the dynamic imine bond exchange kinetics by taking part in noncovenant interactions and that a higher amine concentration is beneficial to decreasing the activated energy of relaxation of the vanillin-PDMS polyimines.[24] As discussed above, excess amines are present in the final products in this study. Under the stimulation of unreacted amines, the polyimines were repairable *via* imine exchange and metathesis.

The proposed reactions during repair are displayed in Figure 9. As for lignin-OAm polyimines, unreacted ketones in modified lignin further condense with excess amines in the OAm to form imine bonds. Meanwhile, lignin-OAm polyimine molecules exchange imine bonds and metathesize with amines in unreacted OAm under pressure reversibly (Figure 9a). As for lignin-PDMS polyimines, unreacted ketones in modified lignin are likely stimulated to condense with free PDMS *via* heat and pressure. Simultaneously, imine exchange reactions occurred among the existing and newly formed imine bonds, and imine metathesis reactions occurred between imines and uncondensed amines in PDMS or lignin-PDMS polyimines (Figure 9b).

We also admit that there are a couple of limitations in the current study. Firstly, a more precise control of the lignin fractionation to yield several representative lignin chemistry (i.e., MW and functional groups) will be beneficial to further illustrate the MW and ketone grafting density of KL, so that the tailoring effect of lignin will be more underlying to establish a fundamental relationship. Secondly, the repair time is long, which is energy-consuming. Further studies on lignin pretreatment/structural tailoring and application of lignin-PDMS polyimines for coatings are ongoing in our group.

CONCLUSIONS

We have showed that lignin-based polyimines were successfully prepared *via* a catalyst-free Schiff-base reaction between the ketone groups in modified lignins and amine groups in OAm and PDMS. The ketone grafting density of MFL is higher than that of MKL, resulting in a higher M_w of MFL-O and a denser cross-linking network of MFL-P, suggesting lignin fractions with lower MW and more active functional groups are favorable to the synthesis of polyimines. Additionally, lignin-OAm polyimines are linear grafted copolymers with lignin as skeletons and OAm as arms, while lignin-PDMS polyimines are three-dimensional cross-linked polymer networks. The stress−relaxation behaviors of synthesized polyimines indicate the occurrence of transimination under thermal-stress activation. As a result, lignin-OAm polyimines are self-repairable and hot reprocessable, while lignin-PDMS polyimines are repairable with the assistance of a healing agent, heat, and stress. Moreover, lignin-PDMS polyimines exhibit great hydrophobicity, thermal stability, translucency, and UV-blocking ability. MFL-P features better hydrophobicity and light-shielding ability but inferior repairability and translucency because of the intensified cross-linking density and a more rigid network structure. The synthesized lignin-PDMS polyimines appear to have a great potential to be applied for repairable, and hydrophobic coatings.

ASSOCIATED CONTENT

Supporting Information

The Supporting Information is available free of charge at https://pubs.acs.org/doi/10.1021/acssuschemeng.3c08482.

Solvent fractionation of KL into FL; FTIR, ^{1}H NMR, ^{13}C NMR, and ^{31}P NMR spectra of lignin and modified lignin; solid-state NMR spectra of MKL-P and MFL-P; GPC curves of PDMS, lignin, modified lignin, and polyimines; stress−relaxation curves and Arrhenius equation plots of MKL and MFL; reprocessability test for lignin-OAm polyimine films; self-healing ability test for lignin-OAm polyimine films; images of lignin-PDMS polyimine films before and after repair; quantification of hydroxyl groups in lignin and modified lignin determined by ^{31}P NMR (PDF)

AUTHOR INFORMATION

Corresponding Author

Mi Li − *Center for Renewable Carbon, School of Natural Resources, The University of Tennessee, Knoxville, Tennessee 37996, United States;* orcid.org/0000-0001-7523-1266; Email: mli47@utk.edu

Authors

Di Xie − *Center for Renewable Carbon, School of Natural Resources, The University of Tennessee, Knoxville, Tennessee 37996, United States*

Yunqiao Pu − *Joint Institute of Biological Sciences, Bioscience Division, Oak Ridge National Laboratory, Oak Ridge, Tennessee 37831, United States*

Nathan D. Bryant − *Joint Institute of Biological Sciences, Bioscience Division, Oak Ridge National Laboratory, Oak Ridge, Tennessee 37831, United States; Department of*

https://doi.org/10.1021/acssuschemeng.3c08482
ACS Sustainable Chem. Eng. 2024, 12, 6606−6618

Chemical and Biomolecular Engineering, The University of Tennessee, Knoxville, Tennessee 37996, United States

David P. Harper − *Center for Renewable Carbon, School of Natural Resources, The University of Tennessee, Knoxville, Tennessee 37996, United States; Department of Materials Science and Engineering, The University of Tennessee, Knoxville, Tennessee 37996, United States;* orcid.org/0000-0003-2783-5406

Wei Wang − *Department of Mechanical, Aerospace and Biomedical Engineering, The University of Tennessee, Knoxville, Tennessee 37996, United States;* orcid.org/0000-0002-1260-2098

Arthur J. Ragauskas − *Center for Renewable Carbon, School of Natural Resources and Department of Chemical and Biomolecular Engineering, The University of Tennessee, Knoxville, Tennessee 37996, United States; Joint Institute of Biological Sciences, Bioscience Division, Oak Ridge National Laboratory, Oak Ridge, Tennessee 37831, United States;* orcid.org/0000-0002-3536-554X

Complete contact information is available at: https://pubs.acs.org/10.1021/acssuschemeng.3c08482

Author Contributions

D.X. performed conceptualization, methodologies, investigation, formal analysis, data curation, validation, writing of the original draft, review, and editing. Y.P. performed resources acquisition, data curation, review, and editing. N.B. performed investigation, review, and editing. D.H., W.W., and A.R. performed resources acquisition, review, and editing. M.L. performed conceptualization, methodologies, supervision, validation, review and editing, project administration, and funding acquisition.

Notes

The authors declare no competing financial interest.

■ ACKNOWLEDGMENTS

We are grateful for the support from the USDA National Institute of Food and Agriculture, Hatch project 7005828, the South-eastern Regional Sun Grant Centre at the University of Tennessee, and the University of Tennessee Agricultural Experiment Station and AgResearch. The Oak Ridge National Laboratory is managed by UT-Battelle, LLC under Contract DE-AC05-00OR22725 with the U.S. Department of Energy (DOE). The views and opinions of the authors expressed herein do not necessarily state or reflect those of the United States Government or any agency thereof. Neither the United States Government nor any agency thereof, nor any of their employees, makes any warranty, expressed or implied, or assumes any legal liability or responsibility for the accuracy, completeness, or usefulness of any information, apparatus, product, or process disclosed, or represents that its use would not infringe privately owned rights.

■ REFERENCES

(1) Saito, K.; Eisenreich, F.; Türel, T.; Tomović, Ž. Closed-Loop Recycling of Poly(Imine-Carbonate) Derived from Plastic Waste and Bio-based Resources. *Angew. Chem., Int. Ed.* **2022**, *61* (43), No. e202211806.

(2) Adjaoud, A.; Puchot, L.; Federico, C. E.; Das, R.; Verge, P. Lignin-based benzoxazines: A tunable key-precursor for the design of hydrophobic coatings, fire resistant materials and catalyst-free vitrimers. *Chem. Eng. J.* **2023**, *453*, No. 139895.

(3) Wang, Y.; Xu, A.; Zhang, L.; chen, Z.; Qin, R.; Liu, Y.; Jiang, X.; Ye, D.; Liu, Z. Recyclable Carbon Fiber Reinforced Vanillin-Based Polyimine Vitrimers: Degradation and Mechanical Properties Study. *Macromol. Mater. Eng.* **2022**, *307* (7), 2100893.

(4) Zheng, N.; Xu, Y.; Zhao, Q.; Xie, T. Dynamic Covalent Polymer Networks: A Molecular Platform for Designing Functions beyond Chemical Recycling and Self-Healing. *Chem. Rev.* **2021**, *121* (3), 1716−1745.

(5) Belowich, M. E.; Stoddart, J. F. Dynamic imine chemistry. *Chem. Soc. Rev.* **2012**, *41* (6), 2003−2024.

(6) Buzoglu Kurnaz, L.; Bension, Y.; Tang, C. Facile Catalyst-Free Approach toward Fully Biobased Reprocessable Lignin Thermosets. *Macromol. Chem. Phys.* **2023**, *224* (3), 2200303.

(7) Hong, K.; Sun, Q.; Zhang, X.; Fan, L.; Wu, T.; Du, J.; Zhu, Y. Fully Bio-Based High-Performance Thermosets with Closed-Loop Recyclability. *ACS Sustain. Chem. Eng.* **2022**, *10* (2), 1036−1046.

(8) Yang, X.; Ke, Y.; Chen, Q.; Shen, L.; Xue, J.; Quirino, R. L.; Yan, Z.; Luo, Y.; Zhang, C. Efficient transformation of renewable vanillin into reprocessable, acid-degradable and flame retardant polyimide vitrimers. *J. Clean. Prod.* **2022**, *333*, No. 130043.

(9) Häußler, M.; Eck, M.; Rothauer, D.; Mecking, S. Closed-loop recycling of polyethylene-like materials. *Nature.* **2021**, *590* (7846), 423−427.

(10) Geng, H.; Wang, Y.; Yu, Q.; Gu, S.; Zhou, Y.; Xu, W.; Zhang, X.; Ye, D. Vanillin-Based Polyschiff Vitrimers: Reprocessability and Chemical Recyclability. *ACS Sustain. Chem. Eng.* **2018**, *6* (11), 15463−15470.

(11) Li, C.; Ju, B.; Zhang, S. Twin-screw extrusion molding of a cellulose-based vitrimer containing a crosslinkable macromolecular plasticizer. *Int. J. Biol. Macromol.* **2023**, *225*, 1487−1493.

(12) Chong, K. L.; Lai, J. C.; Rahman, R. A.; Adrus, N.; Al-Saffar, Z. H.; Hassan, A.; Lim, T. H.; Wahit, M. U. A review on recent approaches to sustainable bio-based epoxy vitrimer from epoxidized vegetable oils. *Ind. Crop. Prod.* **2022**, *189*, No. 115857.

(13) Li, M.; Pu, Y.; Chen, F.; Ragauskas, A. J. Synthesis and Characterization of Lignin-grafted-poly(ε-caprolactone) from Different Biomass Sources. *New Biotechnol.* **2021**, *60*, 189−199.

(14) Xie, D.; Pu, Y.; Meng, X.; Bryant, N. D.; Zhang, K.; Wang, W.; Ragauskas, A. J.; Li, M. Effect of the Lignin Structure on the Physicochemical Properties of Lignin-Grafted-Poly(ε-caprolactone) and Its Application for Water/Oil Separation. *ACS Sustainable Chem. Eng.* **2022**, *10*, 16882.

(15) Shu, F.; Jiang, B.; Yuan, Y.; Li, M.; Wu, W.; Jin, Y.; Xiao, H. Biological Activities and Emerging Roles of Lignin and Lignin-Based Products: A Review. *Biomacromolecules* **2021**, *22* (12), 4905−4918.

(16) Araújo, L. C. P.; Yamaji, F. M.; Lima, V. H.; Botaro, V. R. Kraft lignin fractionation by organic solvents: Correlation between molar mass and higher heating value. *Bioresour. Technol.* **2020**, *314*, 123757−123757.

(17) Meister, J. J. *Review of the Synthesis, Characterization, and Testing of Graft Copolymers of Lignin*. Vol. 33; Springer: Boston, MA, US, 1986; pp 305−322. DOI: DOI: 10.1007/978-1-4613-2205-4_24.

(18) de Baynast, H.; Tribot, A.; Niez, B.; Audonnet, F.; Badel, E.; Cesar, G.; Dussap, C.-G.; Gastaldi, E.; Massacrier, L.; Michaud, P.; et al. Effects of Kraft lignin and corn cob agro-residue on the properties of injected-moulded biocomposites. *Ind. Crop.Prod.* **2022**, *177*, No. 114421.

(19) Huang, J.; Wang, H.; Liu, W.; Huang, J.; Yang, D.; Qiu, X.; Zhao, L.; Hu, F.; Feng, Y. Solvent-free synthesis of high-performance polyurethane elastomer based on low-molecular-weight alkali lignin. *Int. J. Biol. Macromol.* **2023**, *225*, 1505−1516.

(20) Hao, C.; Liu, T.; Zhang, S.; Brown, L.; Li, R.; Xin, J.; Zhong, T.; Jiang, L.; Zhang, J. A High-Lignin-Content, Removable, and Glycol-Assisted Repairable Coating Based on Dynamic Covalent Bonds. *ChemSusChem* **2019**, *12* (5), 1049−1058.

(21) Huang, J.; Liu, W.; Qiu, X. High Performance Thermoplastic Elastomers with Biomass Lignin as Plastic Phase. *ACS Sustain. Chem. Eng.* **2019**, *7* (7), 6550−6560.

(22) Liu, W.; Fang, C.; Wang, S.; Huang, J.; Qiu, X. High-Performance Lignin-Containing Polyurethane Elastomers with Dynamic Covalent Polymer Networks. *Macromolecules* **2019**, *52* (17), 6474−6484.
(23) Mourdikoudis, S.; Liz-Marzán, L. M. Oleylamine in Nanoparticle Synthesis. *Chem. Mater.* **2013**, *25* (9), 1465−1476.
(24) Bui, R.; Brook, M. A. Thermoplastic silicone elastomers from divanillin crosslinkers in a catalyst-free process. *Green Chem.* **2021**, *23* (15), 5600−5608.
(25) Chen, X.; Guo, T.; Mo, X.; Zhang, L.; Wang, R.; Xue, Y.; Fan, X.; Sun, S. Reduced nutrient release and greenhouse gas emissions of lignin-based coated urea by synergy of carbon black and polysiloxane. *Int. J. Biol. Macromol.* **2023**, *231*, No. 123334.
(26) Huang, K.; Ma, S.; Wang, S.; Li, Q.; Wu, Z.; Liu, J.; Liu, R.; Zhu, J. Sustainable valorization of lignin with levulinic acid and its application in polyimine thermosets. *Green Chem.* **2019**, *21* (18), 4964−4497.
(27) Xie, D.; Pu, Y.; Meng, X.; Bryant, N. D.; Zhang, K.; Wang, W.; Ragauskas, A. J.; Li, M. Effect of the Lignin Structure on the Physicochemical Properties of Lignin-Grafted-Poly(ε-caprolactone) and Its Application for Water/Oil Separation. *ACS Sustain. Chem. Eng.* **2022**, *10* (50), 16882−16895.
(28) Meng, X.; Crestini, C.; Ben, H.; Hao, N.; Pu, Y.; Ragauskas, A. J.; Argyropoulos, D. S. Determination of hydroxyl groups in biorefinery resources via quantitative 31P NMR spectroscopy. *Nat. Protoc.* **2019**, *14* (9), 2627−2647.
(29) Wang, S.; Ma, S.; Li, Q.; Xu, X.; Wang, B.; Huang, K.; liu, Y.; Zhu, J. Facile Preparation of Polyimine Vitrimers with Enhanced Creep Resistance and Thermal and Mechanical Properties via Metal Coordination. *Macromolecules* **2020**, *53* (8), 2919−2931.
(30) Gellerstedt, G. Softwood kraft lignin: Raw material for the future. *Ind. Crop. Prod.* **2015**, *77*, 845−854.
(31) Zhou, B.; Li, J.; Liu, W.; Jiang, H.; Li, S.; Tan, L.; Dong, L.; She, L.; Wei, Z. Functional-Group Modification of Kraft Lignin for Enhanced Supercapacitors. *ChemSusChem* **2020**, *13* (10), 2628−2633.
(32) Song, C.; Gao, C.; Fatehi, P.; Wang, S.; Jiang, C.; Kong, F. Influence of structure and functional group of modified kraft lignin on adsorption behavior of dye. *Int. J. Biol. Macromol.* **2023**, *240*, 124368−124368.
(33) Shorey, R.; Mekonnen, T. H. Esterification of lignin with long chain fatty acids for the stabilization of oil-in-water Pickering emulsions. *Int. J. Biol. Macromol.* **2023**, *230*, No. 123143.
(34) Naseem, A.; Tabasum, S.; Zia, K. M.; Zuber, M.; Ali, M.; Noreen, A. Lignin-derivatives based polymers, blends and composites: A review. *Int. J. Biol. Macromol.* **2016**, *93* (Pt A), 296−313.
(35) Guo, H.; Zhu, L.; Dang, C.; Zhao, J.; Dick, B. Synthesis and photophysical properties of ruthenium(ii) polyimine complexes decorated with flavin. *Phys. Chem. Chem. Phys.* **2018**, *20* (25), 17504−17516.
(36) Hong, N.; Yu, W.; Xue, Y.; Zeng, W.; Huang, J.; Xie, W.; Qiu, X.; Li, Y. A novel and highly efficient polymerization of sulfomethylated alkaline lignins via alkyl chain cross-linking method. *Holzforschung* **2016**, *70* (4), 297−304.
(37) Chao, A.; Negulescu, I.; Zhang, D. Dynamic Covalent Polymer Networks Based on Degenerative Imine Bond Exchange: Tuning the Malleability and Self-Healing Properties by Solvent. *Macromolecules* **2016**, *49* (17), 6277−6284.
(38) Duval, A.; Layrac, G.; van Zomeren, A.; Smit, A. T.; Pollet, E.; Avérous, L. Isolation of Low Dispersity Fractions of Acetone Organosolv Lignins to Understand their Reactivity: Towards Aromatic Building Blocks for Polymers Synthesis. *ChemSusChem* **2021**, *14* (1), 387−397.
(39) Chen, X.; Li, Z.; Zhang, L.; Wang, H.; Qiu, C.; Fan, X.; Sun, S. Preparation of a novel lignin-based film with high solid content and its physicochemical characteristics. *Ind. Crop. Prod.* **2021**, *164*, No. 113396.
(40) Wang, Y.-Y.; Li, M.; Wyman, C. E.; Cai, C. M.; Ragauskas, A. J. Fast Fractionation of Technical Lignins by Organic Cosolvents. *ACS Sustain. Chem. Eng.* **2018**, *6* (5), 6064−6072.
(41) Tanadchangsaeng, N.; Yu, J. Thermal stability and degradation of biological terpolyesters over a broad temperature range. *J. Appl. Polym. Sci.* **2015**, *132* (13), 41715.
(42) Sbrescia, S.; Engels, T.; Van Ruymbeke, E.; Seitz, M. Molecular weight effects on the stress-relaxation behavior of soft thermoplastic elastomer by means of temperature scanning stress relaxation (TSSR). *J. Rheol.* **2022**, *66* (6), 1321−1330.
(43) Jones, B. H.; Wheeler, D. R.; Black, H. T.; Stavig, M. E.; Sawyer, P. S.; Giron, N. H.; Celina, M. C.; Lambert, T. N.; Alam, T. M. Stress Relaxation in Epoxy Thermosets via a Ferrocene-Based Amine Curing Agent. *Macromolecules* **2017**, *50* (13), 5014−5024.
(44) Scheutz, G. M.; Lessard, J. J.; Sims, M. B.; Sumerlin, B. S. Adaptable Crosslinks in Polymeric Materials: Resolving the Intersection of Thermoplastics and Thermosets. *J. Am. Chem. Soc.* **2019**, *141* (41), 16181−16196.
(45) Grassia, L.; D'Amore, A. Deconvolution of the segmental and chain modes in amorphous polymers: Do the short-chain modes affect the bulk relaxation. *Polymer* **2021**, *225*, No. 123801.
(46) Elling, B. R.; Dichtel, W. R. Reprocessable Cross-Linked Polymer Networks: Are Associative Exchange Mechanisms Desirable. *ACS Cent. Sci.* **2020**, *6* (9), 1488−1496.
(47) Taynton, P.; Zhu, C.; Loob, S.; Shoemaker, R.; Pritchard, J.; Jin, Y.; Zhang, W. Re-healable polyimine thermosets: Polymer composition and moisture sensitivity. *Polym. Chem.* **2016**, *7* (46), 7052−7056.
(48) Scarica, C.; Suriano, R.; Levi, M.; Turri, S.; Griffini, G. Lignin Functionalized with Succinic Anhydride as Building Block for Biobased Thermosetting Polyester Coatings. *ACS Sustain. Chem. Eng.* **2018**, *6* (3), 3392−3401.
(49) Griffini, G.; Passoni, V.; Suriano, R.; Levi, M.; Turri, S. Polyurethane Coatings Based on Chemically Unmodified Fractionated Lignin. *ACS Sustain. Chem. Eng.* **2015**, *3* (6), 1145−1154.
(50) Lin, M.; Yang, L.; Zhang, H.; Xia, Y.; He, Y.; Lan, W.; Ren, J.; Yue, F.; Lu, F. Revealing the structure-activity relationship between lignin and anti-UV radiation. *Ind. Crop. Prod.* **2021**, *174*, No. 114212.
(51) Xia, Q.; Chen, C.; Yao, Y.; He, S.; Wang, X.; Li, J.; Gao, J.; Gan, W.; Jiang, B.; Cui, M.; et al. In Situ Lignin Modification toward Photonic Wood. *Adv. Mater.* **2021**, *33* (8), No. e2001588.
(52) Sayem, A. S. M.; Simorangkir, R. B. V. B.; Esselle, K. P.; Hashmi, R. M.; Liu, H. A Method to Develop Flexible Robust Optically Transparent Unidirectional Antennas Utilizing Pure Water, PDMS, and Transparent Conductive Mesh. *IEEE T Antenn. Propag.* **2020**, *68* (10), 6943−6952.
(53) Zheng, X.; Yang, H.; Sun, Y.; Zhang, Y.; Guo, Y. A molecular dynamics simulation on self-healing behavior based on disulfide bond exchange reactions. *Polymer* **2021**, *212*, No. 123111.
(54) Urzúa-Leiva, R.; Denis-Alpizar, O. Study of the CN($X_2\Sigma$+) + N(4S) Reaction at High Temperatures: Potential Energy Surface and Thermal Rate Coefficients. *J. Phys. Chem. A* **2021**, *125* (37), 8168−8174.
(55) Kuchma, A. E.; Shchekin, A. K. Regularities of non-stationary diffusion growth of overcritical gas bubbles and kinetics of bubble distribution in presence of capillary and viscous forces. *J. Chem. Phys.* **2021**, *154* (14), 144101.

https://doi.org/10.1021/acssuschemeng.3c08482
ACS Sustainable Chem. Eng. 2024, 12, 6606−6618